



Original scientific paper

Electrochemical sensing platform for simultaneous detection of 6-mercaptopurine and 6-thioguanine using RGO-Cu₂O/Fe₂O₃ modified screen-printed graphite electrode

Fatemeh Irannezhad, Jamileh Seyed-Yazdi[✉] and Hoda Hekmatara

Department of Physics, Faculty of Science, Vali-e-Asr University of Rafsanjan, Rafsanjan, Iran

Corresponding author: [✉]j.seyedyazdi@gmail.com

Received: September 3, 2021; Accepted: October 14, 2021; Published: November 14, 2021

Abstract

A sensitive electrochemical sensor was developed using reduced graphene oxide RGO-Cu₂O/Fe₂O₃ nanocomposite for 6-mercaptopurine detection based on a facile fabrication method. The surface morphology and structural composition of this nanocomposite were evaluated by X-ray diffraction (XRD), field emission scanning electron microscopy (FE-SEM), and Fourier transform infrared (FT-IR) spectroscopy. The screen-printed graphite electrode (SPGE) modified with RGO-Cu₂O/Fe₂O₃ nanocomposite (RGO-Cu₂O/Fe₂O₃/SPGE) indicated excellent electrochemical properties to detect 6-mercaptopurine. The linear dynamic range was estimated between 0.05 and 400.0 μM for 6-mercaptopurine detection, with a limit of detection of 0.03 μM. Also, RGO-Cu₂O/Fe₂O₃/SPGE sensor showed good activity for simultaneous detection of 6-mercaptopurine and 6-thioguanine. In the coexistence system of 6-mercaptopurine and 6-thioguanine, two clear and well-isolated voltammetric peaks were obtained by differential pulse voltammetry (DPV). Additionally, the proposed sensor was examined for applicability by determining 6-mercaptopurine and 6-thioguanine in real samples, and the recovery in the range of 97.5-103.0 % was obtained.

Keywords

electrochemical sensor; reduced graphene oxide; copper(I) oxide; iron(III) oxide

Introduction

6-mercaptopurine (6-MP), a sulfur analog of adenine, was introduced in early 1950 and subsequently applied as a chemotherapy drug to treat childhood and adulthood leukemias [1,2]. Now, it has usually been prescribed as an anti-inflammatory and immunosuppressive agent to manage medical conditions like inflammatory bowel disease (IBD), rheumatoid arthritis, polycythemia, chorioadenoma and choriocarcinoma [3,4]. Nevertheless, some disadvantages limited the use of cytotoxic antitumor 6-MP, such as hepatotoxicity and bone marrow toxicity [5]. 6-MP cannot detect the difference between healthy and cancer cells [6], highlighting the necessity for monitoring doses of this agent in various biological and pharmaceutical media.

6-thioguanine (6-TG) or thiopurine antimetabolite, as an analog of purine nucleosides, was first recognized as a health-promoting agent in the treatment of neoplastic conditions. This cytotoxic agent is extensively applied to treat disorders like acute leukemia, auto-immune disease, and inflammatory bowel disease [7,8]. Nevertheless, high doses of 6-TG are toxic and can lead to serious side effects, such as bone marrow depression, causes myelosuppression, gastrointestinal complications, and liver problems [6,9]. Accordingly, there is a need to develop a facile and sensitive approach to control the 6-TG concentration in various biological and pharmaceutical media.

The administration of 6-MP and 6-TG in treating various cancers such as acute lymphoblastic leukemia at an appropriate and effective dose is of great importance in analytical measurements for both biological and pharmaceutical preparations. Hence, numerous methods have been employed in this regard so far, including high-performance liquid chromatography [10,11], chemiluminescence [12], colorimetric assays [13], surface-enhanced Raman scattering [14], liquid chromatography-tandem mass spectrometry [15,16], and localized surface plasmon resonance [17] for the determination of 6-MP and 6-TG. It should be noted that these techniques, in addition to excellent selectivity and sensitivity, have some disadvantages such as expensiveness, the need for pretreatment, and complicated analysis. Among these, electrochemical analytical techniques have attracted special attention due to their unique properties like simplicity, rapidity, field-based portability, and cost-effectiveness [18-24].

Screen printing is now a facile and easy technique that can be applied in the fabrication and modification of electrochemical sensors [25-27]. This method has been used by researchers to construct stable, reproducible, and disposable electrodes and devices. Among these, a screen-printed electrode (SPE) is a promising candidate for real sample analysis. SPEs have some benefits for produced electrochemical sensors which can perform *in situ* analysis because of unique features, including cost-effectiveness, high availability, linear output, miniaturized morphology, low power, easy to use at ambient temperature, rapid response, and ability to connect to portable devices.

Nevertheless, there are some shortcomings for electrochemical sensitivity, such as huge overpotential, slow electrochemical behavior in detecting different analytes, which might be eliminated using approaches like electrode surface modification to improve interfacial electron transfer in the electroanalysis [28-33]. The electrochemical sensors can benefit from such nano-materials due to cost-effectiveness, large specific surface area, variable morphologies, excellent electrocatalytic properties, and the ability to enhance electron transfer at low overpotentials [34-40].

The given work aimed to produce RGO-Cu₂O/Fe₂O₃ nanocomposite for electrochemical detection of 6-MP, explore the synergistic effects of Fe₂O₃, Cu₂O, and RGO nano-particles, and evaluate sensitivity, the limit of detection, and linear dynamic range of electrocatalyst performance for 6-MP detection. Moreover, this sensor was examined for co-detection of 6-MP and 6-TG. The applicability of the proposed sensor was examined to determine 6-MP and 6-TG in biological and pharmaceutical media.

Experimental

Materials and equipment

All chemicals of analytical grade utilized in the current work belong to Merck and Sigma-Aldrich. Metrohm electrochemical equipment was used to record all electrochemical experiments. DropSens SPGE (DRP-110, Spain) was utilized to carry out the electrochemical tests. The experiments were performed by a three-electrode cell system consisting of 4 mm graphite as a working electrode, a silver pseudo-reference electrode, and graphite used as an auxiliary electrode.

In addition, ortho-phosphoric acid as well as the respective salts (KH_2PO_4 , K_2HPO_4 , K_3PO_4) with pH ranging between 2.0 and 9.0, have been utilized to procure buffer solution. A digital pH meter (Metrohm 710) was recruited to measure all pH values.

Construction of RGO-Cu₂O/Fe₂O₃ nanocomposite

As explained elsewhere, a modified Hummers' method was used to construct graphene oxide (GO) by graphite powder [41,42]. First, 50 mg GO was dispersed in 20 mL ethanol in an ultrasonic bath. Then, iron(III) nitrate nonahydrate and copper(II) nitrate trihydrate with a ratio of 3:7 were added to the mixture and stirred until it turned into a uniform suspension. Subsequently, using sodium hydroxide (6 M) solution, pH was adjusted to 11, and a brown viscous suspension was obtained. The mixture was transferred into a stainless-steel autoclave and then held in an oven at a temperature of 240 °C for 26 hours, followed by centrifuging and washing thoroughly with distilled water and ethanol to set a neutral pH value. At last, the resulting product was dried at 50 °C for 16 hours.

Construction of RGO-Cu₂O/Fe₂O₃/SPGE

The unmodified SPGE was coated with RGO-Cu₂O/Fe₂O₃ nanocomposite. RGO-Cu₂O/Fe₂O₃ nanocomposite stock solution was obtained by adding RGO-Cu₂O/Fe₂O₃ nanocomposite (1 mg) in aqueous solution (1 mL) under ultrasonication for an hour, followed by casting 4 μL aliquot of RGO-Cu₂O/Fe₂O₃ solution on the working electrode, and finally air-drying for 30 min at room temperature.

The surface areas of RGO-Cu₂O/Fe₂O₃/SPGE and bare SPGE were obtained by CV using 1 mM $\text{K}_3\text{Fe}(\text{CN})_6$ at different scan rates. Using the Randles-Sevcik formula [43] for RGO-Cu₂O/Fe₂O₃/SPGE, the electrode surface was found 0.103 cm^2 which was about 3.2 times greater than bare CPE.

Results and discussion

Determination of RGO-Cu₂O/Fe₂O₃ nanocomposite characteristics

The XRD spectrum taken from as-fabricated RGO-Cu₂O/Fe₂O₃ nanocomposite is shown in Figure 1.

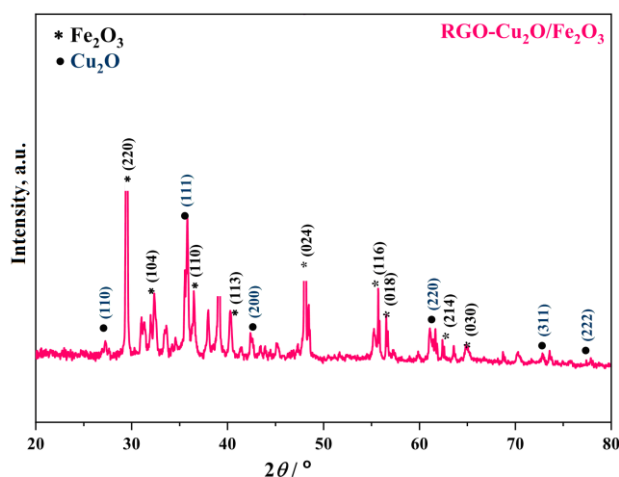


Figure 1. XRD spectrum analysis of synthesized RGO-Cu₂O/Fe₂O₃ nanocomposite

Diffraction peaks of $\alpha\text{-Fe}_2\text{O}_3$ at 29.4, 32.3, 36.5, 40.2, 48.0, 55.5, 56.5 and 64.8° correspond respectively to the crystalline planes (220), (104), (110), (113), (024), (116), (018), (214), and (030). Diffraction peaks of Cu₂O at 27.2, 35.6, 42.2, 61.3, 73.1 and 77.5° correspond respectively to the crystalline planes (110), (111), (200), (220), (311), and (222).

Figure 2 shows the FE-SEM image of the prepared RGO-Cu₂O/Fe₂O₃ nanocomposite. It clearly shows Cu₂O nanoribbons, α -Fe₂O₃ nanoparticles, and graphene oxide layers that formed RGO-Cu₂O/Fe₂O₃ nanocomposite.

Figure 3 shows FT-IR spectrum analysis of the RGO-Cu₂O/Fe₂O₃ nanocomposite. Formation of the nanocomposite, *i.e.*, the presence of Fe-O and Cu-O bonds, is confirmed by peaks at about 833 cm⁻¹. The peaks at about 1465 and 1588 cm⁻¹ are related to C=O and C=C bonds of graphene oxide, respectively, and the bond of 3415 cm⁻¹ to O-H stretching vibration due to adsorbed water molecules.

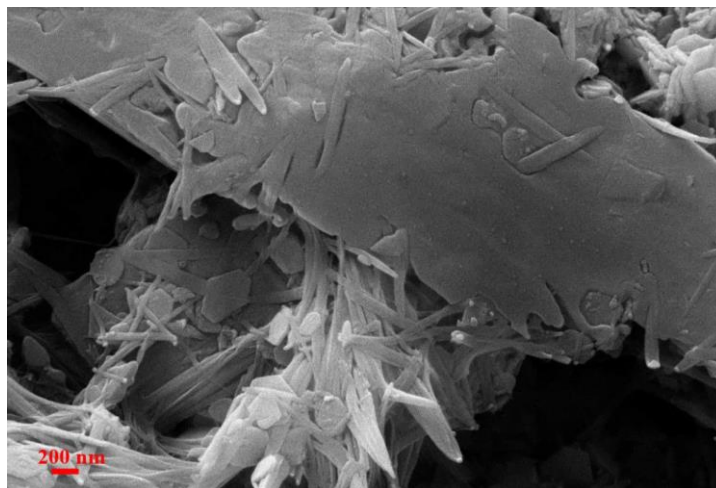


Figure 2. FE-SEM image of synthesized RGO-Cu₂O/Fe₂O₃ nanocomposite

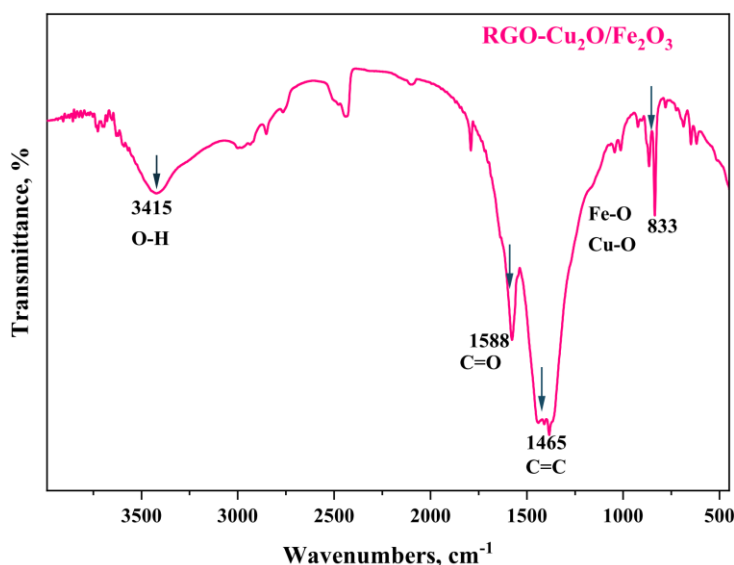
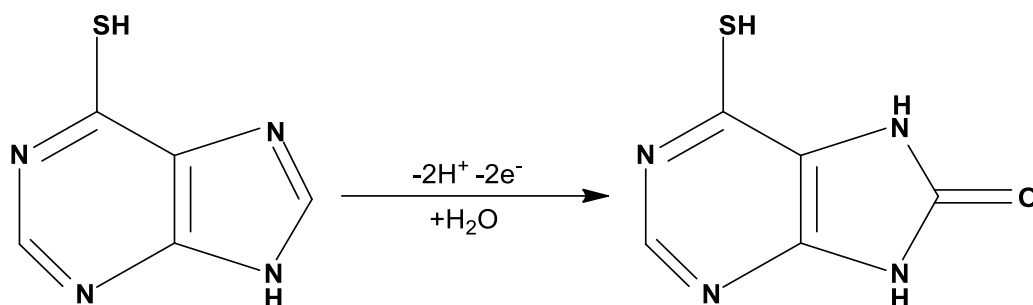


Figure 3. FT-IR spectrum analysis of synthesized RGO-Cu₂O/Fe₂O₃ nanocomposite

Electrochemical behavior of 6-mercaptopurine at RGO-Cu₂O/Fe₂O₃/SPGE

The supporting electrolyte pH showed a significant effect on the electrocatalysis of 6-MP on the surface of RGO-Cu₂O/Fe₂O₃/SPGE (Scheme 1). The impact of pH on 6-MP (100.0 μ M) detection in PBS on the modified electrode surface was evaluated at different pH values of 2.0-9.0. The maximum peak current response of 6-MP was found at the pH value of about 7.0. Hence, we selected pH 7.0 as the optimal experimental condition for experiments.

The electrochemical behavior of 6-MP in PBS at pH 7.0 was studied by cyclic voltammetry (CV) at bare SPGE, and SPGE modified by RGO-Cu₂O/Fe₂O₃, and results are shown in Figure 4. As seen in Figure 4 for unmodified SPGE (curve a), a lower peak current of 6-MP oxidation is observed than for modified SPGE (curve b).



Scheme 1. Electrochemical oxidation mechanism of 6-MP at the surface of the modified electrode

This means a lower sensitivity for 6-MP for bare than for modified SPGE. The voltammogram of 6-MP detection on both electrodes displayed an irreversible oxidation peak, with the elevation of the peak current and reduction of the anodic peak potential value of 6-MP observed for RGO-Cu₂O/Fe₂O₃/SPGE. The optimal electrocatalytic impact for 6-MP oxidation was reported on the RGO-Cu₂O/Fe₂O₃/SPGE surface.

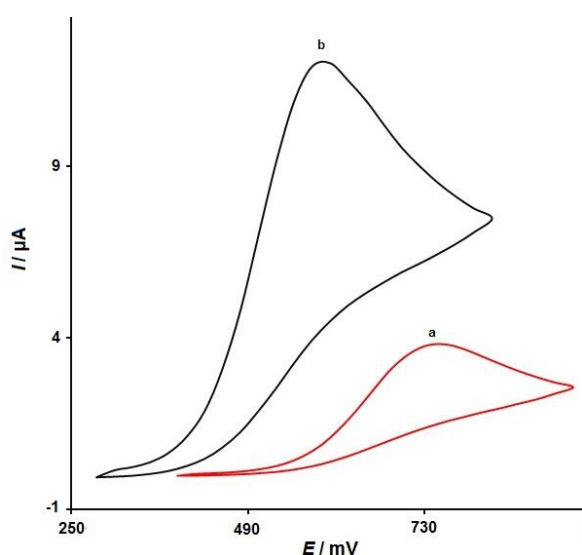


Figure 4. CV responses of 100.0 μM 6-mercaptopurine at (a) bare SPGE and (b) RGO-Cu₂O/Fe₂O₃/SPGE in PBS (0.1 M, pH 7.0)

Scan rate influence

Figure 5 displays the linear sweep voltammetry (LSV) behavior of 100.0 μM 6-MP in PBS of pH 7.0 at variable scan rates (v) on the surface of RGO-Cu₂O/Fe₂O₃/SPGE.

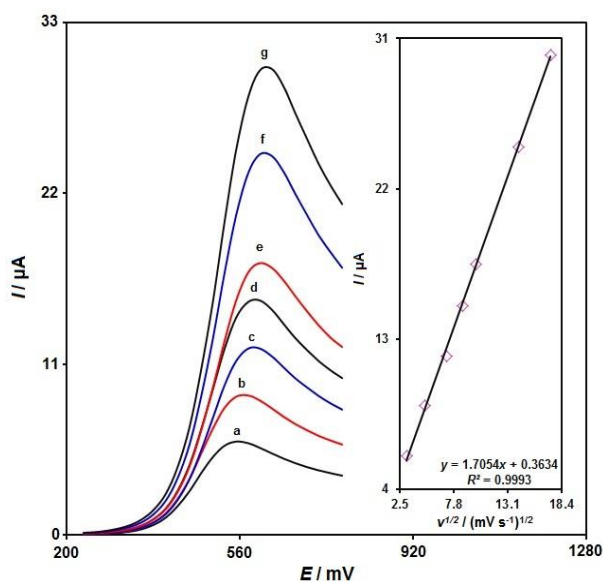


Figure 5. LSV curves of 100.0 μM 6-MP in PBS (0.1 M, pH 7.0) at different scan rates (10 - 300 mV/s) on the surface of RGO-Cu₂O/Fe₂O₃/SPGE (a-g stand for 10, 25, 50, 75, 100.0, 200.0, and 300.0 mV/s). Inset: plot of 6-MP oxidation peak current versus square root of scan rate

There is a gradual elevation in the peak current value of 6-MP oxidation and a positive shift of oxidation peak potential by rising v from 10 to 300 mV/s. According to Figure 5 (inset), the anodic peak current (I_{pa}) of 6-MP is proportional to the square root of scan rate ($v^{1/2}$), and the regression equation (1)

$$I_{pa} = 1.7054 v^{1/2} + 0.3634 \quad (R^2 = 0.9993) \quad (1)$$

Hence, a diffusion-controlled electrochemical reaction of 6-MP at RGO-Cu₂O/Fe₂O₃/SPGE can be assumed.

To provide data about the rate determining step, a Tafel plot was drawn based on data of rising sector related to a current-voltage curve at low scan rate (10 mV/s) for 100.0 μ M 6-MP (Figure 6, inset). The linearity of E versus $\log I$ plot reveals the intervention of electrode process kinetics. In accordance with the slope of this plot, the number of transferred electrons for the rate-determining step can be calculated. The inset in Figure 6 displays the Tafel slope of 0.1133 V for the linear sector. The Tafel slope value means the rate-limiting step related to one-electron transfer, with a transfer coefficient (α) of 0.48.

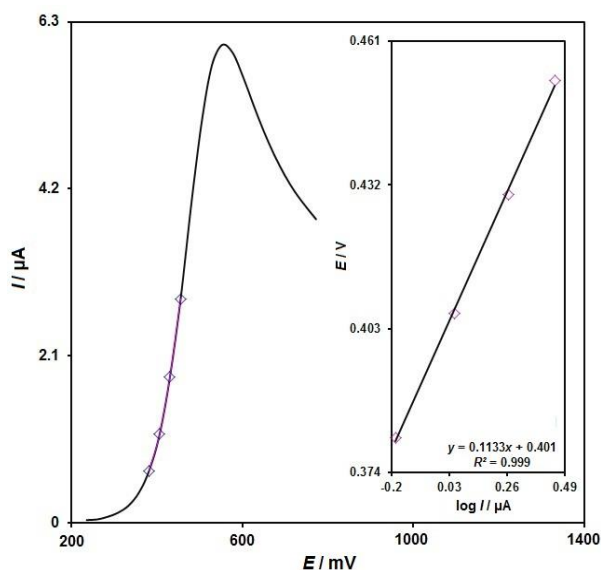


Figure 6. LSV response for 100 μ M 6-MP in PBS (0.1 M, pH 7.0) at the scan rate of 10 mV/s on RGO-Cu₂O/Fe₂O₃/SPGE; inset: Tafel plot of the rising sector of the related voltammogram

Chronoamperometric analysis

Chronoamperometric measurements for 6-MP detection on RGO-Cu₂O/Fe₂O₃/SPGE surface shown in Figure 7 were performed at the potential of 0.65 V and variable 6-MP concentrations in PBS (0.1 M, pH 7.0). The Cottrell equation defines the electrochemical reaction current at the limited condition of mass transport for 6-MP as electroactive material having a certain diffusion coefficient (D) value [43]. Figure 7A displays the experimental plots of I versus $t^{-1/2}$ with the optimal fits at various 6-MP concentrations. Figure 7B shows the slopes of achieved straight lines versus 6-MP concentration. According to the obtained slope and Cottrell equation, the mean D value of 6-MP was calculated as $7.0 \times 10^{-5} \text{ cm}^2/\text{s}$.

DPV analysis of 6-MP on RGO-Cu₂O/Fe₂O₃/SPGE surface

Differential pulse voltammetry (DPV) is a versatile technique for the determination of 6-MP because of its higher sensitivity, and the obtained voltammograms measured for step potential of 0.01 V and pulse amplitude of 0.025 V are shown in Figure 8. Figure 8 shows that with increasing concentration of 6-MP from 0.05 μ M – 400.0 μ M, I_{pa} values increased with slight shifts of oxidation potential values.

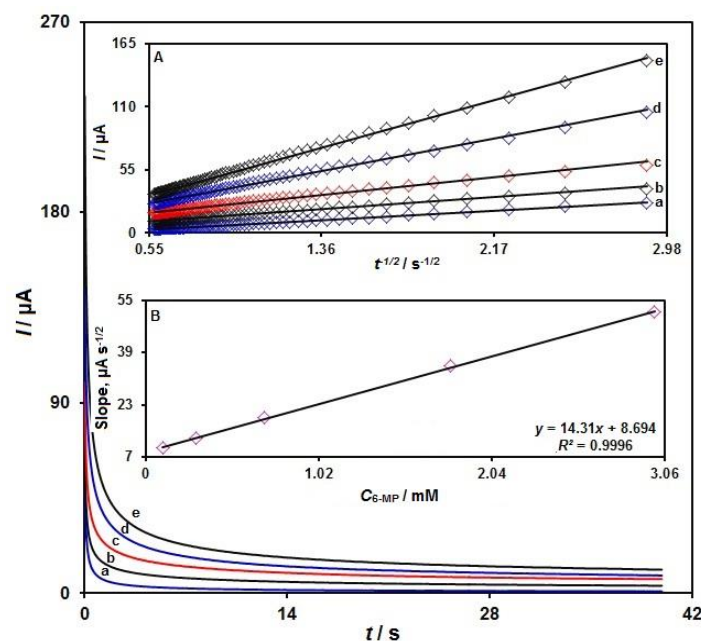


Figure 7. Chronoamperograms obtained for RGO-Cu₂O/Fe₂O₃/SPGE in PBS (0.1 M, pH 7.0) at variable 6-MP concentrations (a–e: 0.1, 0.3, 0.7, 1.8 and 3.0 mM of 6-MP); inset A: plot of I versus $t^{1/2}$ based on chronoamperograms (a – e); inset B: slope plot of straight line versus 6-MP concentration

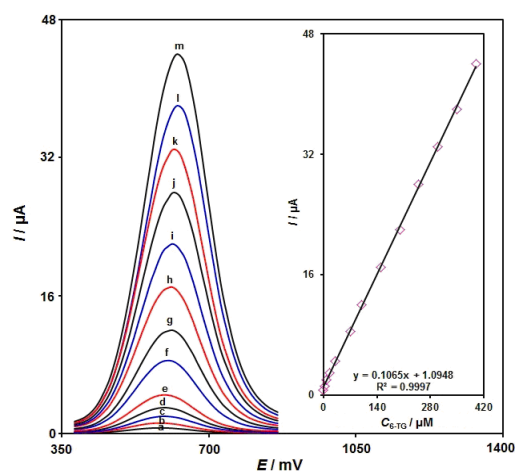


Figure 8. DPV responses of 6-MP on RGO-Cu₂O/Fe₂O₃/SPGE at different concentrations of 6-MP in PBS (0.1 M, pH 7.0) (a–m refer to 0.05, 2.5, 7.5, 15.0, 30.0, 70.0, 100.0, 150.0, 200.0, 250.0, 300.0, 350.0 and 400.0 μ M); inset: calibration curve of DPV peak current against concentration of 6-MP

The plot of I_{pa} versus 6-MP concentration is drawn in the inset of Figure 8, showing a nearly straight line with excellent linearity. The linear regression equation is defined as: $I_{pa} = 0.1065 C_{6-MP} + 1.0948$ ($R^2 = 0.9977$). The equation of $3S_{bl}/m$ was selected to calculate the limit of detection (LOD), where m stands for the slope of the standard plot and S_{bl} for a standard deviation for linearity of blank solution anodic peak current after five determinations. The LOD was estimated as 0.02 μ M.

The analytical performance of the present electrochemical method is in Table 1 compared with those obtained by some other relevant methods for the electrochemical detection of 6-MP.

Table 1. Comparison of linear range and detection limits for 6-MP reported for different electrochemical sensors

Electrochemical sensor	Method	Linear range, μ M	LOD, μ M	Ref.
Multiwall carbon nanotubes paste electrode/carbon paste electrode	Square wave voltammetry (SWV)	0.5–900	0.1	[44]
Cobalt salophen complex/carbon nanotube-paste electrode	DPV	1–100	0.1	[45]
Boron-doped diamond electrode	DPV	1–450	0.51	[46]
RGO-Cu ₂ O/Fe ₂ O ₃ /SPGE	DPV	0.05–400.0	0.03	This work

Simultaneous detection of 6-MP and 6-TG on RGO-Cu₂O/Fe₂O₃/SPGE

DPVs for simultaneous detection of 6-MP and 6-TG using RGO-Cu₂O/Fe₂O₃/SPGE are presented in Figure 9. Two oxidation peaks appear at 0.6 V and 0.75 V for 6-MP and 6-TG, respectively. There is a linear elevation in the peak current intensity for both analytes with the simultaneous enhancement in their contents. Figure 9 (insets A and B) presents the related standard curves for 6-MP and 6-TG. The sensitivity for 6-MP in the simultaneous detection was the same as the single one. Based on these findings, the applicability of simultaneously measuring concentrations of both 6-MP and 6-TG is evident on the RGO-Cu₂O/Fe₂O₃/SPGE surface.

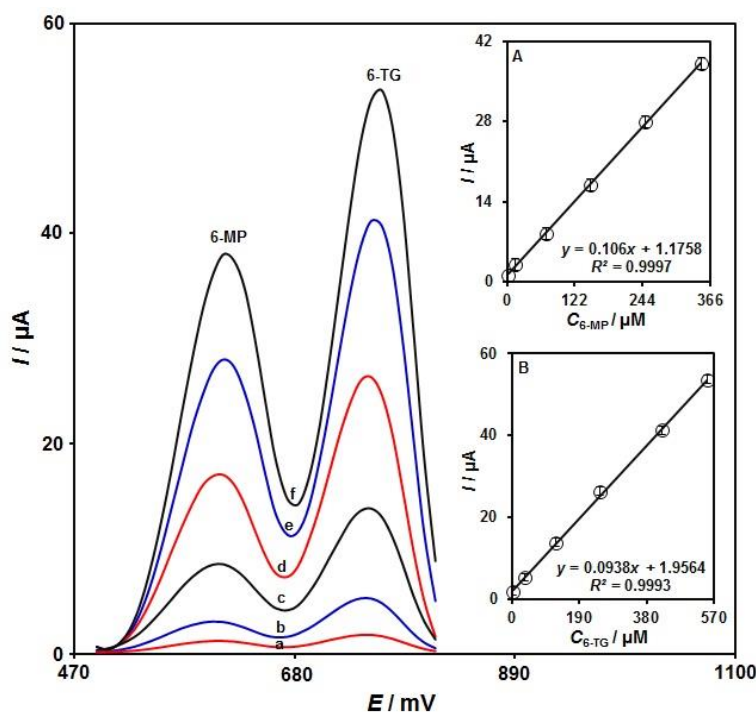


Figure 9. DPVs of RGO-Cu₂O/Fe₂O₃/SPGE in PBS (0.1 M, pH 7.0) at variable 6-MP and 6-TG concentrations (a-f refer to mixed solutions of 2.5 + 3.0, 15.0 + 35.0, 70.0 + 125.0, 150.0 + 250.0, 250.0 + 425.0, and 350.0 + 550.0 μM of 6-MP and 6-TG); inset A: plot of peak currents versus 6-MP concentrations; inset B: plot of peak currents versus 6-TG concentrations

Real sample analysis

The applicability of the prepared RGO-Cu₂O/Fe₂O₃/SPGE sensor was explored *via* detection of 6-MP and 6-TG present in urine specimens, 6-MP tablets, and 6-TG tablets. Table 2 displays the recovery rates of 97.5 to 103.3 % for tested samples. These findings showed the efficiency of the proposed sensor for the detection of 6-MP and 6-TG in real specimens.

Table 2. Determination of 6-MP and 6-TG in real specimens (n=5).

Sample	C / μM				Recovery, %		RSD, %	
	Spiked		Found		6-MP	6-TG	6-MP	6-TG
Urine	0	0	-	-	-	-	-	-
	5.0	6.0	4.9	6.2	98.0	103.3	2.8	2.9
	7.5	8.0	7.6	7.8	101.3	97.5	3.1	1.7
6-mercaptopurine tablet	0	0	7.0	-	-	-	3.5	-
	1.0	5.5	7.8	5.6	97.5	101.8	2.7	3.0
	2.0	6.5	9.3	6.4	103.3	98.5	2.1	2.4
6-thioguanine Tablet	0	0	-	7.5	-	-	-	2.9
	4.5	1.0	4.6	8.3	102.2	97.6	1.7	2.4
	8.5	2.0	8.6	9.6	96.5	101.1	2.9	3.2

Conclusion

In this work, RGO-Cu₂O/Fe₂O₃ nanocomposite was prepared by a facile method and applied for construction of RGO-Cu₂O/Fe₂O₃/SPGE sensor for electrochemical detection of 6-mercaptopurine. The proposed sensor is easy to use without complicated preparations prior to 6-mercaptopurine detection. The developed sensor showed a linear electrochemical response to 6-mercaptopurine ranging from 0.05 to 400.0 μM, providing the limit of detection of 0.03 μM. Also, the oxidation peaks of 6-mercaptopurine and 6-thioguanine can be entirely separated with a clear peak potential difference of 0.15 V, which allowed simultaneous determination of two drugs. Finally, the applicability of the as-fabricated RGO-Cu₂O/Fe₂O₃/SPGE sensor was verified by detections of 6-mercaptopurine and 6-thioguanine in real samples.

References

- [1] Y. Su, Y. Y. Hon, Y. Chu, M. E. Van de Poll, M. V. Relling, *Journal of Chromatography B: Biomedical Sciences and Applications* **732** (1999) 459-468. [https://doi.org/10.1016/s0378-4347\(99\)00311-4](https://doi.org/10.1016/s0378-4347(99)00311-4)
- [2] J. A. Montgomery, *Progress in Medicinal Chemistry* **7** (1970) 69-123.
- [3] S. Sahasranaman, D. Howard, S. Roy, *European Journal of Clinical Pharmacology* **64** (2008) 753-767. <https://doi.org/10.1007/s00228-008-0478-6>
- [4] O. Nielsen, B. Vainer, J. Rask-Madsen, *Alimentary Pharmacology & Therapeutics* **15** (2001) 1699-1708. <https://doi.org/10.1046/j.1365-2036.2001.01102.x>
- [5] F. H. Rashidy, S. M. Ragab, A. A. Dawood, S. A. Temraz, *Menoufia Medical Journal* **28** (2015) 411-414. <https://doi.org/10.4103/1110-2098.163930>
- [6] E. Petit, S. Langouet, H. Akhdar, C. Nicolas-Nicolaz, A. Guillouzo, E. Morel, *Toxicology in Vitro* **22** (2008) 632-642. <https://doi.org/10.1016/j.tiv.2007.12.004>
- [7] B. Meijer, C. J. J. Mulder, G. J. Peters, A. A. van Bodegraven, N. K. H. de Boer, *World Journal of Gastroenterology* **22** (2016) 9012-9021. <https://doi.org/10.3748/wjg.v22.i40.9012>
- [8] R. Rajashekaraiyah, P. R. Kumar, N. Prakash, G. S. Rao, V. R. Devi, M. Metta, H. D. Narayanaswamy, M. N. Swamy, K. Satyanarayan, S. Rao, D. Rathnamma, A. Sahadev, U. Sunilchandra, C. R. Santhosh, H. Dhanalakshmi, S. N. Kumar, S. W. Ruban, G. P. Kalmath, A. R. Gomes, K. R. A. Kumar, P. K. Govindappa, *International Journal of Biological Macromolecules* **148** (2020) 704-714. <https://doi.org/10.1016/j.ijbiomac.2020.01.117>
- [9] A. Vora, C. D. Mitchell, L. Lennard, T. O. B. Eden, S. E. Kinsey, J. Lilleyman, S. M. Richards, *The Lancet* **368** (2006) 1339-1348. [https://doi.org/10.1016/S0140-6736\(06\)69558-5](https://doi.org/10.1016/S0140-6736(06)69558-5)
- [10] H. Mawatari, Y. Kato, S. Nishimura, N. Sakura, K. Ueda, *Journal of Chromatography B* **716** (1998) 392-396. [https://doi.org/10.1016/S0378-4347\(98\)00329-6](https://doi.org/10.1016/S0378-4347(98)00329-6)
- [11] G. Cangemi, A. Barabino, S. Barco, A. Parodi, S. Arrigo, G. Melioli, *International Journal of Immunopathology* **25** (2012) 435-444. <https://doi.org/10.1177/039463201202500213>
- [12] P. Biparva, S. M. Abedirad, S. Y. Kazemi, *Spectrochimica Acta, Part A: Molecular and Biomolecular Spectroscopy* **145** (2015) 454-460. <https://doi.org/10.1016/j.saa.2015.03.019>
- [13] K. A. Rawat, R. K. Singhal, S. K. Kailasa, *Sensors & Actuators, B: Chemical* **249** (2017) 30-38. <https://doi.org/10.1016/j.snb.2017.04.018>
- [14] H. Li, X. Chong, Y. Chen, L. Yang, L. Luo, B. Zhao, Y. Tian, *Colloids and Surfaces A: Physicochemical and Engineering Aspects* **493** (2016) 52-58. <https://doi.org/10.1016/j.colsurfa.2016.01.032>
- [15] S. Supandi, Y. Harahap, H. Harmita, R. Andalusia, M. Ika, *Asian Journal of Pharmaceutical and Clinical Research* **10** (2017) 120-125. <http://dx.doi.org/10.22159/ajpcr.2017.v10i9.19790>

- [16] J. H. Jacobsen, K. Schmiegelow, J. Nersting, *Journal of Chromatography B-Analytical Technologies in the Biomedical and Life Sciences* **881** (2012) 115-118. <https://doi.org/10.1016/j.ichromb.2011.11.032>
- [17] N. Bi, M. Hu, H. Zhu, H. Qi, Y. Tian, H. Zhang, *Spectrochimica Acta, Part A: Molecular and Biomolecular Spectroscopy* **107** (2013) 24-30. <https://doi.org/10.1016/j.saa.2013.01.014>
- [18] J. I. Gowda, M. Mallappa, S. T. Nandibewoor, *Sensing and Bio-Sensing Research* **12** (2017) 1-7. <https://doi.org/10.1016/j.sbsr.2016.11.002>
- [19] B. Hatamluyi, Z. Es'haghi, *Electrochimica Acta* **283** (2018) 1170-1177. <https://doi.org/10.1016/j.electacta.2018.07.068>
- [20] D. N. Unal, E. Eksin, A. Erdem, *Analytical Letters* **51** (2018) 265-278. <https://doi.org/10.1080/00032719.2017.1338714>
- [21] M. Pirozmand, A. Nezhadali, M. Payehghadr, L. Saghatforoush, *Eurasian Chemical Communications* **2** (2020) 1021-1032. <https://doi.org/10.22034/ECC.2020.241560.1063>
- [22] A. Khodadadi, E. Faghieh-Mirzaei, H. Karimi-Maleh, A. Abbaspourrad, S. Agarwal, V. K. Gupta, *Sensors & Actuators, B: Chemical* **284** (2019) 568-574. <https://doi.org/10.1016/j.snb.2018.12.164>
- [23] S. M. Patil, V. P. Pattar, S. T. Nandibewoor, *Journal of Electrochemical Science and Engineering* **6** (2016) 265-276. <https://doi.org/10.5599/jese.350>
- [24] P. Prasad, N. Y. Sreedhar, *Chemical Methodologies* **2** (2018) 277-290. <https://doi.org/10.22034/CHEMM.2018.63835>
- [25] N. Jaiswal, I. Tiwari, C. W. Foster, C. E. Banks, *Electrochimica Acta* **227** (2017) 255. <https://doi.org/10.1016/j.electacta.2017.01.007>
- [26] N. Jaiswal, I. Tiwari, *Analytical Methods* **9** (2017) 3895-3907. <https://doi.org/10.1039/C7AY01276D>
- [27] I. Tiwari, M. Singh, M. Gupta, J. P. Metters, C. E. Banks, *Analytical Methods* **7** (2015) 2020-2027. <https://doi.org/10.1039/C4AY02271H>
- [28] H. Karimi-Maleh, F. Karimi, Y. Orooji, G. Mansouri, A. Razmjou, A. Aygun, F. Sen, *Scientific Reports* **10** (2020) 11699. <https://doi.org/10.1038/s41598-020-68663-2>
- [29] A. A. S. Mou, A. Ouarzane, M. El Rhazi, *Journal of Electrochemical Science and Engineering* **7** (2017) 111-118. <https://doi.org/10.5599/jese.386>
- [30] Y. Zhang, X. Li, D. Li, Q. Wei, *Colloids and Surfaces B: Biointerfaces* **186** (2020) 110683. <https://doi.org/10.1016/j.colsurfb.2019.110683>
- [31] F. Mehri-Talarposhti, A. Ghorbani-Hasan Saraei, L. Golestan, S. A. Shahidi, *Asian Journal of Nanosciences and Materials* **3** (2020) 313-320. <https://doi.org/10.26655/AJNANOMAT.2020.4.5>
- [32] C. Chen, Z. Han, W. Lei, Y. Ding, J. Lv, M. Xia, Q. Hao, *Journal of Electrochemical Science and Engineering* **9** (2019) 143-152. <https://doi.org/10.5599/jese.630>
- [33] H. Karimi-Maleh, M. Lütfi Yola, N. Atar, Y. Orooji, F. Karimi, P. Senthil Kumar, J. Rouhi, M. Baghayeri, *Journal of Colloid and Interface Science* **592** (2021) 174-185. <https://doi.org/10.1016/j.jcis.2021.02.066>
- [34] J. Ghodsi, A. A. Rafati, Y. Shoja, *Advanced Journal of Chemistry-Section A* **1** (2018) 39-55. <https://doi.org/10.29088/SAMI/AJCA.2018.5.3955>
- [35] S. Mohajeri, A. Dolati, K. Yazdanbakhsh, *Journal of Electrochemical Science and Engineering* **9** (2019) 207-222. <https://doi.org/10.5599/jese.666>
- [36] H. Karimi-Maleh, K. Cellat, K. Arıkan, A. Savk, F. Karimi, F. Şen, *Materials Chemistry and Physics* **250** (2020) 123042. <https://doi.org/10.1016/j.matchemphys.2020.123042>
- [37] W. H. Elobeid, A. A. Elbashir, *Progress in Chemical and Biochemical Research* **2** (2019) 24-33. <https://doi.org/10.33945/SAMI/PCBR.2019.2.2433>

- [38] H. Zhao, H. Ma, X. Li, B. Liu, R. Liu, S. Komarneni, *Applied Clay Science* **200** (2021) 105907. <https://doi.org/10.1016/j.clay.2020.105907>
- [39] H. Karimi-Maleh, F. Karimi, S. Malekmohammadi, N. Zakariae, R. Esmaili, S. Rostamnia, M. Lütfi Yola, N. Atar, S. Movaghgharnezhad, S. Rajendran, A. Razmjou, Y. Orooji, S. Agarwal, V. K. Gupta, *Journal of Molecular Liquids* **310** (2020) 113185. <https://doi.org/10.1016/j.molliq.2020.113185>
- [40] K. Roja, P. R. Prasad, P. Sandhya, N. Y. Sreedhar, *Journal of Electrochemical Science and Engineering* **6** (2016) 253-263. <https://doi.org/10.5599/jese.349>
- [41] M. Darvishi, M. Jamali-Paghaleh, F. Jamali-Paghaleh, J. Seyed-Yazdi, *Materials Research Express* **4** (2017) 016501. <https://doi.org/10.1088/2053-1591/aa52cf>
- [42] M. Darvishi, J. Seyed-Yazdi, *Surfaces and Interfaces* **4** (2016) 1-8. <https://doi.org/10.1016/j.surfin.2016.07.001>
- [43] A. J. Bard, L.R. Faulkner, *Electrochemical Methods: Fundamentals and Applications*, John Wiley & Sons, New York, 2nd edition, 2001.
- [44] M. Keyvanfard, V. Khosravi, H. Karimi-Maleh, K. Alizad, B. Rezaei, *Journal of Molecular Liquids* **177** (2013) 182-189. <https://doi.org/10.1016/j.molliq.2012.10.020>
- [45] S. Shahrokhian, F. Ghorbani-Bidkorbeh, A. Mohammadi, R. Dinarvand, *Journal of Solid State Electrochemistry* **16** (2012) 1643-1650. <https://doi.org/10.1007/s10008-011-1575-5>
- [46] M. Hanko, L. Švorc, A. Planková, P. Mikuš, *Journal of Electroanalytical Chemistry* **840** (2019) 295-304. <https://doi.org/10.1016/j.jelechem.2019.03.067>

